

Original Research

Correlation Analysis Between 3D and Plane DAT Binding Parameters of ¹¹C-CFT PET/CT and the Clinical Characteristics of Patients with Parkinson's Disease

Xiaodong Wu^{1,2,†}, Ziyuan Li^{1,†}, Jing Gan^{3,†}, Feng Wei¹, Ping Wu⁴, Sheng Liang¹, Yufei Ma¹, Lin Ding¹, Chuantao Zuo⁴, Zhenguo Liu^{3,*}, Hui Wang^{1,*}, Yafu Yin^{1,*}

Submitted: 3 May 2024 Revised: 23 December 2024 Accepted: 31 December 2024 Published: 25 April 2025

Abstract

Objective: The aim of this study was to investigate the correlation between dopamine transporter (DAT) positron emission tomography (PET)/computed tomography (CT) and the clinical characteristics and rating scales of Parkinson's disease (PD) patients. Additionally, we sought to assess the scientific validity and feasibility of integrating 3D-dopaminergic binding parameters into the clinical scoring system for PD. **Methods**: A total of 75 patients with PD who underwent ¹¹C-methyl-N-2β-methyl ester-3β-(4-fluorophenyl) tropane (11C-CFT) PET/CT from April, 2019 to June, 2021 were retrospectively analyzed. Clinical characteristics, including age, sex, and disease duration, as well as the modified Hoehn-Yahr (H-Y) scale, Unified Parkinson's Disease Rating Scale (UPDRS) parts II and III (II-III), and Mini-Mental State Examination (MMSE) scores of PD patients during the corresponding time periods were collected. DAT binding parameters and their derived parameters based on plane and 3D images in the neostriatum were analyzed for consistency with plane and 3D parameters, and the correlation between DAT parameters and the clinical features of patients were assessed using SPSS software. Results: The DAT binding parameters derived from 3D images demonstrated good consistency with the plane parameters (p < 0.05). The asymmetry index (ai) of DAT binding parameters based on 3D and plane images showed good consistency in the anterior putamen (p < 0.05). The plane parameters of the anterior and posterior putamen were statistically correlated with the UPDRS II-III score and H-Y score of PD patients (p < 0.05), whereas those of the caudate nucleus were correlated with UPDRS II and MMSE scores. The 3D parameters in the neostriatum showed good statistical correlation with disease duration, UPDRS II-III score, H-Y score, and H-Y stage of PD patients (p < 0.05), and the ai was significantly correlated with MMSE score (p < 0.05). The 3D parameters in the putamen and posterior putamen exhibited significant statistical correlation with the UPDRS II-III score, H-Y score, and H-Y stage in PD patients (p < 0.05). The ai in the putamen showed statistical correlation with UPDRS III and MMSE scores, and the ai in the posterior putamen showed statistical correlation with UPDRS II score (p < 0.05). Conclusions: Quantitative parameters based on plane and 3D images of ¹¹C-CFT PET/CT showed good consistency. Moreover, 3D parameters in the neostriatum had a stronger correlation with activities of daily living, UPDRS motor scores, disease severity and duration, and cognition compared with plane parameters in PD patients.

Keywords: Parkinson's disease; ¹¹C-CFT; PET/CT; plane parameter; 3D parameter

1. Background

Parkinson's disease (PD) is a degenerative disorder of the central nervous system due to the degeneration of dopaminergic neurons in the substantia nigra and the subsequent dopamine deficiency in the striatum [1]. The prevalence among the elderly is as high as 3.3%. PD is characterized by high prevalence, high disability, progressive aggravation, insidious onset, and poor prognosis. The patients' survival period is significantly shortened, and they often succumb to various complications such as pneumonia and urinary tract infection [2–4]. Therefore, timely and ac-

curate diagnosis of PD, along with effective symptomatic treatment, is crucial for improving patients' quality of life, reducing the occurrence of complications, and effectively prolonging survival. There is no specific diagnostic method for PD. The clinical diagnosis of PD mainly relies on medical history, clinical manifestations and physician expertise. The golden standard for diagnosis is the identification of PD-specific pathological changes (Lewy bodies) in brain tissue sections obtained through pathological biopsy. As known, pathological biopsy is an invasive examination that is challenging due to difficulties in obtaining tissue sam-

 $^{^{1}} Department of Nuclear Medicine, Xinhua Hospital, Shanghai Jiao Tong University School of Medicine, 200092 Shanghai, China Chi$

²Department of Radiology, Shandong Cancer Hospital and Institute, Shandong First Medical University and Shandong Academy of Medical Sciences, 250000 Jinan, Shandong, China

³Department of Neurology, Xinhua Hospital, Shanghai Jiao Tong University School of Medicine, 200092 Shanghai, China

⁴PET Center, Hua Shan Hospital, Fudan University, 200040 Shanghai, China

^{*}Correspondence: liuzhenguo@xinhuamed.com.cn (Zhenguo Liu); wanghui@xinhuamed.com.cn (Hui Wang); yinyafu@xinhuamed.com.cn; yinyf-2001@163.com (Yafu Yin)

[†]These authors contributed equally. Academic Editor: Gernot Riedel

ples, affected by the location and quantity of the materials, and is often not well tolerated by patients [5,6]. Thus, there is a critical need for a non-invasive, easy-to-use, objective, sensitive, and specific diagnostic method for PD.

As a molecular probe of positron emission tomography (PET), 11 C-methyl-N-2 β -methyl ester-3 β -(4fluorophenyl) tropane (11C-CFT) specifically binds to the presynaptic membrane dopamine transporter (DAT), which could reflect the function of dopaminergic neurons in the substantia nigra-striatal pathway [7–9]. Normal DAT neuroimaging is one of the diagnostic criteria for ruling out PD, and DAT imaging, particularly the quantitative analysis, is useful to understand the relationship between early dopaminergic dysfunction and clinical manifestation in PD [10,11]. In current quantitative analysis of DAT PET/Computed Tomography (CT), the most commonly used parameter is the average standardized uptake value (SUVavg) in the standardized regions of interest (ROIs) of the caudate and putamen [4], which is used to calculate relative indices such as dopamine receptor binding index (DBI) or asymmetry index (Dai) in each hemisphere. DBI belongs to the plane parameter since it is based on the SUV in ROI of tomography image. The parameters derived from 3D images can provide information on the volume and amount of radiopharmaceuticals, and have been widely used in tumor research [12–14]. However, at present, the 3D parameters about the amount of DAT binding are rarely used. The neostriatum (including caudate and putamen) has a relatively well-defined anatomical region, making it suitable for the delineation of 3D parameters.

In this study, we measured and analyzed the 3D parameter, specifically the volume and total binding amount of DAT in the caudate and putamen. We also examined the consistency between 3D and plane parameters and their correlation with disease duration, modified Hoehn and Yahr (H-Y) scale, the unified Parkinson's disease rating scale (UPDRS) II and III scores, and Mini-Mental State Examination (MMSE) in PD patients.

2. Materials and Methods

2.1 Patients

According to the following inclusion and exclusion criteria, from April 2019 to June 2021, 75 PD patients were retrospectively included in this study, who underwent ¹¹C-CFT PET/CT at the Department of Nuclear Medicine, Xinhua Hospital Affiliated to Shanghai Jiao Tong University School of Medicine. Inclusion criteria: (1) The patients were diagnosed with PD by 2 neurologists according to the "Diagnostic Criteria for Brain Bank of the Parkinson's Society of London, UK" [15]; (2) The patients' clinical data and scales were complete, reliable and clear. Exclusion criteria: (1) Non-primary PD; (2) Presence of other brain diseases, such as stroke in the neostriatum, which might affect the uptake of ¹¹C-CFT.

Anti-parkinsonian medications were withdrawn for more than 12 hours before clinical evaluation and imaging acquisition. The clinical assessment for individual patient was conducted using the UPDRS II-III [16], modified H-Y scale and MMSE. All patients were classified into different stages according to the H-Y scale. The study was approved by the Ethics Committee of Xinhua Hospital Affiliated to Shanghai Jiao Tong University School of Medicine. All research was performed in accordance with relevant guidelines/regulations. The study was carried out in accordance with the guidelines of the Declaration of Helsinki. All patients gave written informed consent before ¹¹C-CFT PET/CT scanning.

2.2 11 C-CFT PET/CT Imaging

PET/CT examinations were performed on a Biograph 64 system (Siemens Healthineers, BIOGRAPHM CT/S, Erlangen, Germany) with a 21.6 cm axial field of view. ¹¹C-CFT was injected intravenously with a dose of 8–15 mCi, which was produced by chemists from the Nuclear Medicine Department of Shanghai Jiao Tong University School of Medicine using the Sumitomo HM-10 cyclotron and Sumitomo Carbon-11 multifunctional synthesis module (radiochemical purity >90%). About 60–80 minutes after injection, a 20-minute brain PET/CT scan was performed in 3D mode. PET/CT images in the transverse, sagittal, and coronal planes were obtained using an iterative reconstruction algorithm with a thickness of 5 mm, and attenuation correction of CT images.

2.3 Imaging Processing and Data Analysis

All images were analyzed by two experienced nuclear medicine physicians who were blinded to the clinical diagnosis. Plane image-based DAT parameters were obtained through semi-automatic software processing as described previously [17]. In brief, SPM software (version 5, Statistical Parametric Mapping; Wellcome Department of Imaging Neuroscience, Institute of Neurology, London, UK) implemented in Matlab7.4 (Mathworks Inc., Sherborn, MA, USA) and ScanVP software Version 5.9.1 (Centre for Neuroscience, the Feinstein Institute for Medical Research, Manhasset, NY, USA) were used for data processing [18,19]. All images were spatially normalized into Montreal Neurological Institute (MNI) brain space with 3D transformations. A Gaussian filter of 10 mm full width at half maximum was adopted for smoothing the normalized PET images.

Then, on the mean image summed over central slices [20], the standard ROIs were drawn in the caudate nucleus, anterior and posterior putamen, and occipital cortex (as reference) to calculate the regional DAT bindings, plane parameter, which was named as DAT binding of caudate nucleus (DBC), DAT binding of anterior putamen (DBAP) and DAT binding of posterior putamen (DBPP), respectively. ¹¹C-CFT PET is a crucial tool for DAT imaging,



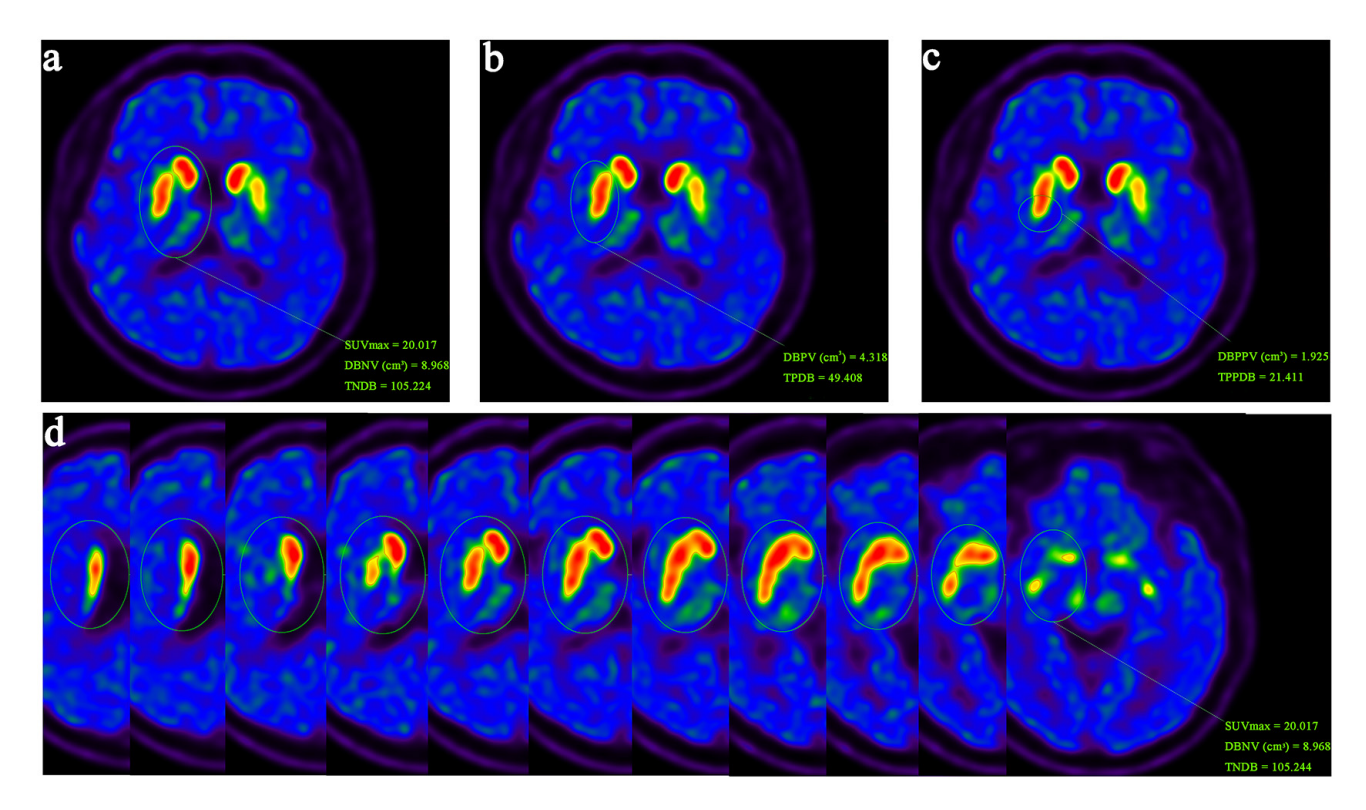


Fig. 1. An illustration example of delineating 3D parameters. First, draw a 3D-ROI in the neostriatum. Taking 40% of SUVmax in the neostriatum region as the threshold, delineate the ROIs in the left and right neostriatum (a), putamen (b) and posterior putamen (c), respectively, and then the effective binding volume and total binding amount of DAT are obtained. (d) 3D-ROI in the neostriatum with each layer display. ROI, regions of interest; SUVmax, maximum standardized uptake value; DAT, dopamine transporter; DBNV, DAT binding volume of neostriatum; TNDB, Total binding amount of DAT in neostriatum; DBPV, DAT binding volume of putamen; TPDB, Total binding amount of DAT in posterior putamen; TPDB, Total binding amount of DAT in posterior putamen.

as it specifically binds to the striatum, while the occipital lobe exhibits hardly uptake of this specific imaging agent. Consequently, we used the occipital lobe as the reference region [21]. The following formula was used: (SUVavg of ROI- SUVavg of occipital lobe)/SUVavg of occipital lobe. Furthermore, the DAT binding asymmetry index of the caudate, anterior and posterior putamen (Cai, APai and PPai) were calculated: the difference between the left and right parameters divided by the average of the left and right parameters.

The 3D parameters were directly obtained using TrueD software (VE 13A, Siemens, Erlangen, Germany), without the need for further imaging processing and were easy to execute. In fact, our image sketching process adopted a semi-automated approach. Firstly, manually draw a circular 3D ROI with an appropriate diameter in the corresponding area of the cross-sectional slice of the PET image. The software would provide various semi quantitative indicator values for this area, such as maximum standardized uptake value (SUVmax). Before conducting this study, we performed extensive testing and comparisons on numerous images and determined that when the threshold was set at 40% of SUVmax, the software could automat-

ically and accurately delineate areas with ¹¹C-CFT functionality within the manually defined 3D ROI. We used this threshold to manually delineate the left and right neostriatum (the whole caudate nucleus and putamen), putamen and posterior putamen, respectively. After that, the software would automatically give the volume of DAT in the corresponding region that effectively binded ¹¹C-CFT. These indicators reflected the functional volume of the neostriatum. At the same time, the software would automatically calculate the total binding amount of DAT to ¹¹C-CFT (Total binding amount of DAT in neostriatum (TNDB), Total binding amount of DAT in putamen (TPDB) and Total binding amount of DAT in posterior putamen (TPPDB)) in the above regions. These indicators could better reflect the residual function of the neostriatum, and also relatively balanced the anatomical volume difference of the human brain (Fig. 1). Finally, the asymmetry index (ai) of the regions were calculated according to the formula as mentioned above for plane parameters. For each 3D parameter, the mean value and the lower value of the left and right regions were selected for analysis, respectively, and any value was with statistical significance, the parameter would be considered to be statistically significant.



2.4 Statistical Analysis

Data were expressed as the mean \pm SD. Bivariate correlation linear analysis was used to analyze the consistency of 3D parameters and plane parameters. Similarly, bivariate correlation linear analysis was also used to correlate DAT binding parameters with clinical data and scores. Pearson's correlation coefficient (r^2) was used to measure the degree of consistency or correlation. Bonferroni was adopted to the correction of multiple comparisons. An independent sample t-test was used to compare the difference of imaging parameters between H-Y early stage and lately stage groups. p < 0.05 was considered statistically significant. SPSS 21.0 Windows software (IBM Corp., Armonk, NY, USA) was used for statistical analysis.

3. Results

3.1 Patients' Clinical Characteristics

The clinical and demographic characteristics of all 75 (40 males, 35 females; 64 ± 10 years) PD patients were listed in Table 1. The average duration of disease of 75 patients was 3.3 ± 2.7 years (0.5–17 years). The average UPDRS II and III scores of 75 patients were 10 ± 7 , 19 ± 12 . The average modified H-Y scale scores of 75 patients were 2 ± 0.8 , including 27 patients in stage 1, 7 in stage 1.5, 27 in stage 2, 12 in stage 3 and 2 in stage 4. Patients with H-Y scores of 1, 1.5 and 2 were defined as early course of disease (n = 61), and patients with H-Y scores of 3 and 4 were defined as late course of disease (n = 14). The average MMSE scores of 75 patients were 27 ± 3 .

3.2 Consistency Analysis of Volume Parameters and Plane Parameters of ¹¹C-CFT PET/CT

The 3D parameters of DAT PET/CT imaging were mostly consistent with the plane parameters (Table 2). The binding volume and total binding amount of DAT in neostriatum and putamen were statistically consistent with DBAP (Bonferroni Corrected p < 0.05, $r^2_{DBNVlower} = 0.286$, $r^2_{DBNVmean} = 0.251, r^2_{TNDBlower} = 0.363, r^2_{TNDBmean} = 0.362,$ $r^2_{DBPVlower} = 0.292, r^2_{DBPVmean} = 0.265, r^2_{TPDBlower} = 0.446,$ $r^2_{TPDBmean} = 0.454$). The binding volume and total binding amount of DAT in putamen and post putamen were statistically consistent with DBPP (Bonferroni Corrected p < $0.05, r^2_{\text{TPDBlower}} = 0.421, r^2_{\text{TPDBmean}} = 0.421, r^2_{\text{TPPDBlower}} =$ 0.544, $r^2_{TPPDBmean} = 0.510$). Similarly, the asymmetry index of binding volumes and total binding amount of DAT in neostriatum and putamen were statistically consistent with APai (Bonferroni Corrected p < 0.05, $r^2_{DBNVai} = 0.254$, $r^2_{TNDBai} = 0.254$, $r^2_{DBPVai} = 0.321$, $r^2_{TPDBai} = 0.439$). The asymmetry index of the total DAT binding amount in putamen was consistent with PPai in statistics (Bonferroni Corrected p < 0.05, $r^2_{TPDBai} = 0.369$).

Table 1. Clinical and demographic characteristics of PD patients.

Variable	Value (Mean ± SD)						
Gender							
Male	40						
Female	35						
Age (years)	$64 \pm 10 \ (25 - 83)$						
Course of disease (years)	$3.3 \pm 2.7 (0.5 – 17)$						
Modified Hoehn and Yahr score	2 ± 0.8						
Modified H-Y grade							
1	27						
1.5	7						
2	27						
Early course	61						
3	12						
4	2						
Late course	14						
UPDRS							
II	$10 \pm 7 (1 35)$						
III	$19 \pm 12 \ (3-54)$						
MMSE	$27 \pm 3 \ (10 – 38)$						

PD, Parkinson's disease; H-Y, Hoehn and Yahr; UPDRS, The unified Parkinson's disease rating scale; MMSE, Mini-Mental State Examination.

3.3 Correlation Between Plane Parameters of DAT Binding and Clinical Data and Scales of PD Patients

DBC was negatively correlated with UPDRS II and positively correlated with MMSE in statistics (Bonferroni Corrected p < 0.05, $r^2_{\text{UPDRS II}} = 0.095$, $r^2_{\text{MMSE}} = 0.099$, Table 3). DBAP was negatively correlated with UPDRS II-III, modified H-Y score in statistics (Bonferroni Corrected p < 0.05, $r^2_{\text{UPDRS II}} = 0.102$, $r^2_{\text{UPDRS III}} = 0.117$, $r^2_{\text{modified H-Y score}} = 0.123$, Table 3). But DBPP was only negatively correlated with modified H-Y score in statistics (Bonferroni Corrected p < 0.05, $r^2 = 0.118$, Table 3). The difference of DBAP between early and late H-Y course was statistically significant (p < 0.05, Table 3). None of the asymmetry index of plane parameters was correlated with the clinical characteristics.

3.4 Correlation Between 3D Parameters of DAT Binding and Clinical Data and Scales of PD Patients

The binding volume and total binding amount of DAT in all regions were negatively correlated with UPDRS II in statistics (Bonferroni Corrected p < 0.05, $r^2_{DBNVlower} = 0.160$, $r^2_{DBNVmean} = 0.160$, $r^2_{DBNVmean} = 0.115$, $r^2_{TNDBlower} = 0.115$, $r^2_{TPDBmean} = 0.118$, $r^2_{DBPVlower} = 0.131$, $r^2_{DBPVmean} = 0.112$, $r^2_{TPDBlower} = 0.124$, $r^2_{TPDBmean} = 0.128$, $r^2_{DBPVlower} = 0.121$, $r^2_{DBPVmean} = 0.081$, Table 3). The binding volume and total binding amount of DAT in all regions were negatively correlated with UPDRS III (Bonferroni Corrected p < 0.05, $r^2_{DBNVlower} = 0.117$, $r^2_{DBNVmean} = 0.109$, $r^2_{TNDBlower} = 0.115$, $r^2_{TNDBmean} = 0.109$, $r^2_{TNDBlower} = 0.115$, $r^2_{TNDBmean} = 0.109$, $r^2_{TNDBlower} = 0.115$, $r^2_{TNDBmean} = 0.109$



Table 2. Consistency analysis of 3D parameters and plane parameters of 11C-CFT PET/CT imaging.

			Plane parameters									
	Variable	Value	DB.	AP	DB	PP	AF	ai ai	PPai			
	variable	value	p	r^2	p	r^2	p	r^2	p	r^2		
	DBNVlower	6.075 ± 2.415	0.026*	0.286	0.096	0.229						
	DBNVmean	6.661 ± 2.421	0.030*	0.251	0.074	0.207						
	DBNVai	0.195 ± 0.178					0.028*	0.254	0.530	0.074		
	TNDBlower	45.297 ± 25.328	0.001*	0.363	0.053	0.224						
	TNDBmean	49.180 ± 25.632	0.001*	0.362	0.058	0.220						
	TNDBai	0.177 ± 0.158					0.000*	0.464	0.054	0.255		
	DBPVlower	0.350 ± 1.410	0.022*	0.292	0.008*	0.328						
	DBPVmean	2.842 ± 1.468	0.044*	0.265	0.012*	0.315						
2D manamatana	DBPVai	0.350 ± 0.2573					0.010*	0.321	0.082	0.236		
3D parameters	TPDBlower	16.148 ± 11.418	0.000*	0.446	0.000* 0.421							
	TPDBmean	19.230 ± 11.885	0.000*	0.454	0.000*	0.421						
	TPDBai	0.351 ± 0.262					0.000*	0.439	0.002*	0.369		
	DBPPVlower	0.740 ± 0.607			0.001*	0.374						
	DBPPVmean	0.926 ± 0.666			0.003*	0.342						
	DBPPVai	0.466 ± 0.389							0.316	0.117		
	TPPDBlower	4.569 ± 4.136			0.000*	0.544						
	TPPDBmean	5.712 ± 4.565			0.000*	0.510						
	TPPDBai	0.470 ± 0.397							0.061	0.217		

^{*:} statistically significant. p-value corrected by Bonferroni < 0.05.

0.113, $r^2_{DBPVlower} = 0.111$, $r^2_{DBPVmean} = 0.093$, $r^2_{TPDBlower} = 0.127$, $r^2_{TPDBmean} = 0.123$, $r^2_{TPPDBlower} = 0.094$, $r^2_{TPPDBmean} = 0.097$, Table 3). The binding volume of DAT in neostriatum and putamen were negatively correlated with modified H-Y score in statistics ($r^2_{DBNVlower} = 0.099$, $r^2_{DBNVmean} = 0.111$, $r^2_{DBPVlower} = 0.096$, $r^2_{DBPVmean} = 0.112$, Table 3) and the total binding amount of DAT in putamen and post putamen were negatively correlated with modified H-Y score in statistics ($r^2_{TPDBlower} = 0.089$, $r^2_{TPDBmean} = 0.121$, $r^2_{TPPDBmean} = 0.083$) (Bonferroni Corrected p < 0.05, Table 3). All these 3D parameters in patients with H-Y early course were significantly bigger than those with late course (p < 0.05). In addition, the DAT binding volume in neostriatum were negatively correlated with the disease duration in statistics (Bonferroni Corrected p < 0.05, $r^2_{DBNVmean} = 0.098$, Table 3).

Among various asymmetry indexes, DAT binding volume of posterior putamen asymmetry index (DBPPVai) and TPPDBai were positively correlated with UPDRS II (${\bf r^2}_{\rm DBPPVai}=0.066,~{\bf r^2}_{\rm TPPDBai}=0.068,~{\bf Table}$ 3), TPDBai was positively correlated with UPDRS III in statistics (${\bf r^2}=0.237$) (Bonferroni Corrected p<0.05, Table 3). Interestingly, the statistics showed MMSE was negative correlation with two asymmetry indexes, including DAT binding vol-

ume of neostriatum asymmetry index (DBNVai), TNDBai (Bonferroni Corrected p < 0.05, $r^2_{DBNVai} = 0.134$, $r^2_{TNDBai} = 0.105$, Table 3).

4. Discussion

As PD is a degenerative disease due to degeneration of dopaminergic neurons and dopamine deficiency in the striatum [22], DAT imaging is widely used in the diagnosis of PD because it can assess the functional state of dopamine neurons in substantia nigra and striatum [23,24]. Previous studies have indicated that DAT intake in PD patients gradually declines with the progress of the disease and the severity of clinical symptoms [24–26]. Using DAT imaging to measure the binding index is a feasible approach to reflect the quantity and distribution of DAT in the striatum.

Although previous studies have given inconsistent results [27–30], some have shown a correlation between UP-DRS motor score and the mean uptake in the neostriatum and putamen, there was no significant difference was observed when compared with caudate uptake alone. Others demonstrated a correlation between both the stage and severity of PD and the caudate-to-putamen ratios. Overall, studies have shown that DAT binding imaging is associated with UPDRS motor score, disease severity [17] and dura-



 $^{^{11}}$ C-CFT, 11 C-methyl-N-2 β -methyl ester-3 β -(4-fluorophenyl) tropane; PET, positron emission tomography; CT, Computed Tomography; DAT, dopamine transporter; DBNV, DAT binding volume of neostriatum; ai, asymmetry index; TNDB, Total binding amount of DAT in neostriatum; DBPV, DAT binding volume of putamen; TPDB, Total binding amount of DAT in putamen; DBPPV, DAT binding volume of posterior putamen; TPPDB, Total binding amount of DAT in posterior putamen; DBAP, DAT binding of anterior putamen; DBPP, DAT binding of posterior putamen; APai, asymmetry index of anterior putamen; PPai, asymmetry index of posterior putamen; 2 , Pearson's correlation coefficient; --, the correlation between these two factors was not studied.

Table 3. Correlation between quantitative parameters of ¹¹C-CFT PET/CT imaging and clinical characteristics and scale scores of patients with PD.

	Variable	Value	Disease	duration	UPDRS II		UPDRS III		Modified H-Y score		Modified H-Y course			MMSE	
	variable		p	r^2	p	r^2	p	r^2	p	r^2	Early course	Late course	p	p	r^2
3D parameters	DBNVlower	6.075 ± 2.415	0.072	0.062	0.000*	0.167	0.012*	0.117	0.028*	0.099	6.510	4.488	0.005*	0.096	0.039
	DBNVmean	6.661 ± 2.421	0.024*	0.098	0.004*	0.160	0.016*	0.109	0.016*	0.111	7.102	5.070	0.005*	0.266	0.017
	DBNVai	0.195 ± 0.178	0.462	0.007	0.138	0.031	0.094	0.038	0.516	0.006	0.178	0.254	0.170	0.001*	0.134
	TNDBlower	45.297 ± 25.328	0.228	0.020	0.012*	0.115	0.009*	0.115	0.126	0.006	46.000	28.950	0.001*	0.062	0.048
	TNDBmean	49.180 ± 25.632	0.144	0.029	0.009*	0.118	0.016*	0.113	0.066	0.073	50.010	32.380	0.001*	0.082	0.042
	TNDBai	0.177 ± 0.158	0.201	0.022	0.247	0.019	0.057	0.049	0.988	0.000	0.167	0.229	0.208	0.005*	0.105
	DBPVlower	0.350 ± 1.410	0.062	0.047	0.006*	0.131	0.012*	0.111	0.024*	0.096	2.638	1.501	0.007*	0.228	0.020
	DBPVmean	2.842 ± 1.468	0.088	0.070	0.012*	0.112	0.032*	0.093	0.016*	0.112	3.084	1.958	0.011*	0.518	0.006
	DBPVai	0.350 ± 0.2573	0.551	0.005	0.072	0.045	0.070	0.061	0.958	0.000	0.317	0.438	0.146	0.056	0.066
	TPDBlower	16.148 ± 11.418	0.280	0.016	0.009*	0.124	0.003*	0.127	0.033*	0.089	18.200	8.533	0.003*	0.135	0.031
	TPDBmean	19.230 ± 11.885	0.153	0.028	0.006*	0.128	0.006*	0.123	0.009*	0.121	21.370	11.170	0.003*	0.169	0.027
	TPDBai	0.351 ± 0.262	0.397	0.010	0.138	0.031	0.042*	0.056	0.576	0.004	0.324	0.429	0.196	0.099	0.038
	DBPPVlower	0.740 ± 0.607	0.102	0.036	0.009*	0.121	0.057	0.074	0.057	0.076	0.820	0.405	0.024*	0.439	0.008
	DBPPVmean	0.926 ± 0.666	0.053	0.051	0.033*	0.088	0.063	0.072	0.072	0.070	1.010	0.594	0.040*	0.805	0.001
	DBPPVai	0.466 ± 0.389	0.788	0.001	0.029*	0.066	0.281	0.016	0.443	0.008	0.431	0.629	0.092	0.166	0.027
	TPPDBlower	4.569 ± 4.136	0.420	0.009	0.012*	0.111	0.021*	0.094	0.051	0.079	5.142	2.197	0.020*	0.282	0.016
	TPPDBmean	5.712 ± 4.565	0.265	0.017	0.033*	0.008	0.021*	0.097	0.042*	0.083	6.344	3.188	0.024*	0.417	0.009
	TPPDBai	0.470 ± 0.397	0.661	0.003	0.027*	0.068	0.288	0.016	0.586	0.004	0.432	0.629	0.102	0.136	0.031
Plane parameters	DBC	0.995 ± 0.429	0.662	0.003	0.018*	0.095	0.087	0.040	0.201	0.023	0.999	0.850	0.236	0.014*	0.099
	DBAP	0.822 ± 0.283	0.389	0.010	0.018*	0.102	0.009*	0.117	0.009*	0.123	0.848	0.666	0.033*	0.060	0.049
	DBPP	0.471 ± 0.210	0.226	0.020	0.144	0.055	0.057	0.074	0.009*	0.118	0.478	0.400	0.215	0.323	0.117
	Cai	0.214 ± 0.244	0.529	0.005	0.088	0.041	0.570	0.005	0.650	0.003	0.205	0.286	0.290	0.962	0.000
	APai	0.230 ± 0.184	0.371	0.011	0.441	0.008	0.343	0.013	0.863	0.000	0.227	0.274	0.419	0.403	0.010
	PPai	0.270 ± 0.207	0.996	0.000	0.544	0.005	0.462	0.008	0.050	0.054	0.272	0.243	0.646	0.067	0.046

^{*:} statistically significant. *p*-value corrected by Bonferroni < 0.05.

DBNV, DAT binding volume of neostriatum; ai, asymmetry index; TNDB, Total binding amount of DAT in neostriatum; DBPV, DAT binding volume of putamen; TPDB, Total binding amount of DAT in putamen; DBPV, DAT binding of caudate nucleus; DBAP, DAT binding of anterior putamen; DBPP, DAT binding of posterior putamen; UPDRS, The unified Parkinson's disease rating scale; H-Y, Hoehn and Yahr; MMSE, Mini-Mental State Examination; Cai, asymmetry index of caudate nucleus; r², Pearson's correlation coefficient.



tion [30] in PD patients. These findings imply that DAT imaging with quantitative parameter has a good capacity in monitoring severity and progression of PD.

In this ¹¹C-CFT PET/CT study involving 75 PD patients, we analyzed the correlation between the quantitative parameters of DAT binding and patients' clinical characteristics, and evaluated the ability of DAT imaging in reflecting the severity and duration of disease, as well as activities of daily living, motor symptoms and cognition. Volumebased 3D PET/CT parameters have been widely used in the diagnosis and prognostic evaluation of tumor lesions, such as the tumor metabolic volume (MTV) and the total amount of glycolysis in the lesion (TLG) in 2'-deoxy-2'-[18F] fluoro-D-glucose ([18F] FDG) PET/CT [12-14, 31,32]. Numerous clinical studies have demonstrated that 3D quantitative parameter in PET/CT imaging offer more precise diagnostic efficacy and prognostic evaluation compared to plane parameter like SUV [13,14]. Therefore, in terms of imaging parameters, we used plane parameters and 3D parameters to explore their correlation with the clinical characteristics of PD, which has been rarely addressed in the previous nervous system imaging research. The results revealed that 3D parameters exhibited good consistency with the plane parameters, and demonstrated a more robust correlation with the clinical characteristics compared to the plane parameters.

There was a significant correlation between 3D parameters in the neostriatum and the duration and severity of disease, activities of daily living, motor symptoms and cognition. Notably, the DAT binding volume of the neostriatum was significantly correlated with the activities of daily living, UPDRS motor score, the severity and duration of disease in PD patients. For example, the longer a patient suffered from PD, the smaller the volume of the neostriatum in his/her brain that could bind with ¹¹C-CFT [33–35]. And the smaller the volume of the neostriatum that could bind with ¹¹C-CFT, the less uptake of ¹¹C-CFT, indicating poorer motor and cognitive function in the patient [35]. Interestingly, the asymmetry of degeneration in the bilateral striatum of patients also impacts their cognitive function.

All studies about DAT imaging with quantitative analysis (plane parameter) were performed based on some specific software tools, statistical parametric mapping (SPM) combined with ScanVP software [4], Neurostat [24], and so on, since ROI delineated manually was variable and with poor repeatability. Not to mention that not all hospitals have these specific software tools, the use of these software is time-consuming and laborious, making widespread clinical application challenging. In contrast, 3D parameters of PET/CT imaging can be easily conducted without the need of imaging processing and the software is simple and could be obtained easily if a PET/CT system is available in the hospital. In addition, the delineation of 3D parameters has good objectivity and repeatability.

This study also has several limitations. Firstly, we did not include normal controls in the study. Secondly, the age group of patients we included was between 65–83 years old. Physiological aging can also cause the differences in the binding of ¹¹C-CFT in elderly patients, but due to sample size limitations, we did not further stratify patients based on physiological age. Regarding cognition, only MMSE was adopted for the correlation analysis with quantitative parameters of DAT PET/CT in this study, and a more detailed assessment of cognitive function is needed to draw more accurate conclusions. Additionally, more data, especially from multiple centers, are required to validate the results. We hope to address these limitations in future research.

5. Conclusions

We investigated the correlation between plane and 3D parameters of DAT binding in PET/CT using ¹¹C-CFT, and the relationship between these quantitative parameters of DAT binding and the clinical features of PD. Our findings indicate that 3D parameters in the neostriatum demonstrate a stronger correlation with the activities of daily living, UP-DRS motor score, the severity and duration of disease and cognition compared to plane parameters in PD patients. Additionally, 3D parameters of DAT imaging have the characteristics of easy operation and high objectivity. Therefore, we recommend using the DAT binding volume in the neostriatum for routine DAT quantitative analysis in clinical practice.

Abbreviations

DAT, Dopamine transporter; PD, Parkinson's disease; H-Y, Hoehn-Yahr; UPDRS, The unified Parkinson's disease rating scale; MMSE, Mini-Mental State Examination; ai, Asymmetry index; PET, Positron emission computed tomography; 11 C-CFT, 11 C-methyl-N-2 β -methyl ester-3 β -(4-fluorophenyl) tropane; SUVavg, Average standardized uptake value; ROIs, Regions of interest; DBI, Dopamine receptor binding index; Dai, Asymmetry index of dopamine receptor binding; SPM5, Statistical Parametric Mapping; MNI, Montreal Neurological Institute; C, caudate nucleus; AP, Anterior putamen; PP, Posterior putamen; DBC, DAT binding of caudate nucleus; DBAP, DAT binding of anterior putamen; DBPP, DAT binding of posterior putamen; N, Neostriatum; DBNV, DAT binding volume of neostriatum; DBPV, DAT binding volume of putamen; DBPPV, DAT binding volume of posterior putamen; TNDB, Total binding amount of DAT in neostriatum; TPDB, Total binding amount of DAT in putamen; TPPDB, Total binding amount of DAT in posterior putamen.

Availability of Data and Materials

The datasets generated during and/or analyzed during the current study are available from the corresponding author on reasonable request.



Author Contributions

Concept and design: YY, HW, ZgL. Acquisition, analysis, or interpretation of data: XW, FW, JG, ZyL. Clinical data providing: JG and ZgL; Analyze the plane parameter data in this study: PW and CZ; Produced CFT and provided a description of the radiopharmaceutical in the article: SL, YM and LD. Drafting of the manuscript: XW and YY. Critical revision of the manuscript for important intellectual content: YY, HW. Statistical analysis: XW and FW. All authors contributed to editorial changes in the manuscript. All authors read and approved the final manuscript. All authors have participated sufficiently in the work and agreed to be accountable for all aspects of the work.

Ethics Approval and Consent to Participate

The study was approved by the Ethics Committee of Xinhua Hospital Affiliated to Shanghai Jiao Tong University School of Medicine. The ethical approval number is XHEC-C-2015-022-2. The study was performed in accordance with the ethical standards as laid down in the 1964 Declaration of Helsinki and its later amendments or comparable ethical standards. Our study obtained written informed consent from all participants.

Acknowledgment

We thank all the participants and their families.

Funding

This work was supported by the National Nature Science Foundation of China (No. 81974270. No. 82472014) and Shanghai Science and Technology Commission (22Y11904100).

Conflict of Interest

The authors declare no conflict of interest.

References

- [1] Klingelhoefer L, Reichmann H. Pathogenesis of Parkinson disease—the gut-brain axis and environmental factors. Nature Reviews. Neurology. 2015; 11: 625–636. https://doi.org/10.1038/nrneurol.2015.197.
- [2] Ashok AH, Mizuno Y, Volkow ND, Howes OD. Association of Stimulant Use With Dopaminergic Alterations in Users of Cocaine, Amphetamine, or Methamphetamine: A Systematic Review and Meta-analysis. JAMA Psychiatry. 2017; 74: 511–519. https://doi.org/10.1001/jamapsychiatry.2017.0135.
- [3] Tang H, Huang J, Nie K, Gan R, Wang L, Zhao J, *et al.* Cognitive profile of Parkinson's disease patients: a comparative study between early-onset and late-onset Parkinson's disease. The International Journal of Neuroscience. 2016; 126: 227–234. https://doi.org/10.3109/00207454.2015.1010646.
- [4] Liu FT, Ge JJ, Wu JJ, Wu P, Ma Y, Zuo CT, et al. Clinical, Dopaminergic, and Metabolic Correlations in Parkinson Disease: A Dual-Tracer PET Study. Clinical Nuclear Medicine. 2018; 43: 562–571. https://doi.org/10.1097/RLU.0000000000002148.
- [5] Hansen AK, Damholdt MF, Fedorova TD, Knudsen K, Parbo P, Ismail R, et al. In Vivo cortical tau in Parkinson's disease using

- 18F-AV-1451 positron emission tomography. Movement Disorders: Official Journal of the Movement Disorder Society. 2017; 32: 922–927. https://doi.org/10.1002/mds.26961.
- [6] Kang Y, Henchcliffe C, Verma A, Vallabhajosula S, He B, Kothari PJ, et al. 18F-FPEB PET/CT Shows mGluR5 Upregulation in Parkinson's Disease. Journal of Neuroimaging: Official Journal of the American Society of Neuroimaging. 2019; 29: 97–103. https://doi.org/10.1111/jon.12563.
- [7] Stoessl AJ, Martin WW, McKeown MJ, Sossi V. Advances in imaging in Parkinson's disease. The Lancet. Neurology. 2011; 10: 987–1001. https://doi.org/10.1016/S1474-4422(11) 70214-9.
- [8] Brooks DJ. Molecular imaging of dopamine transporters. Ageing Research Reviews. 2016; 30: 114–121. https://doi.org/10.1016/j.arr.2015.12.009.
- [9] Stoessl AJ. Neuroimaging in Parkinson's disease: from pathology to diagnosis. Parkinsonism & Related Disorders. 2012; 18 Suppl 1: S55–S59. https://doi.org/10.1016/S1353-8020(11) 70019-0.
- [10] Cummings JL, Henchcliffe C, Schaier S, Simuni T, Waxman A, Kemp P. The role of dopaminergic imaging in patients with symptoms of dopaminergic system neurodegeneration. Brain: a Journal of Neurology. 2011; 134: 3146–3166. https://doi.org/10.1093/brain/awr177.
- [11] Fazio P, Svenningsson P, Forsberg A, Jönsson EG, Amini N, Nakao R, et al. Quantitative Analysis of ¹⁸F-(E)-N-(3-Iodoprop-2-Enyl)-2β-Carbofluoroethoxy-3β-(4'-Methyl-Phenyl) Nortropane Binding to the Dopamine Transporter in Parkinson Disease. Journal of Nuclear Medicine: Official Publication, Society of Nuclear Medicine. 2015; 56: 714–720. https://doi.org/10.2967/jnumed.114.152421.
- [12] Burger IA, Casanova R, Steiger S, Husmann L, Stolzmann P, Huellner MW, et al. 18F-FDG PET/CT of Non-Small Cell Lung Carcinoma Under Neoadjuvant Chemotherapy: Background-Based Adaptive-Volume Metrics Outperform TLG and MTV in Predicting Histopathologic Response. Journal of Nuclear Medicine: Official Publication, Society of Nuclear Medicine. 2016; 57: 849–854. https://doi.org/10.2967/jnumed.115.167684.
- [13] Kostakoglu L, Mattiello F, Martelli M, Sehn LH, Belada D, Ghiggi C, et al. Total metabolic tumor volume as a survival predictor for patients with diffuse large B-cell lymphoma in the GOYA study. Haematologica. 2022; 107: 1633–1642. https://doi.org/10.3324/haematol.2021.278663.
- [14] Dall'Olio FG, Marabelle A, Caramella C, Garcia C, Aldea M, Chaput N, et al. Tumour burden and efficacy of immune-checkpoint inhibitors. Nature Reviews. Clinical Oncology. 2022; 19: 75–90. https://doi.org/10.1038/s41571-021-00564-3.
- [15] Gibb WR, Lees AJ. The relevance of the Lewy body to the pathogenesis of idiopathic Parkinson's disease. Journal of Neurology, Neurosurgery, and Psychiatry. 1988; 51: 745–752. https://doi.org/10.1136/jnnp.51.6.745.
- [16] Fahn S, Oakes D, Shoulson I, Kieburtz K, Rudolph A, Lang A, et al. Levodopa and the progression of Parkinson's disease. The New England Journal of Medicine. 2004; 351: 2498–2508. https://doi.org/10.1056/NEJMoa033447.
- [17] Wen MC, Chan LL, Tan LCS, Tan EK. Depression, anxiety, and apathy in Parkinson's disease: insights from neuroimaging studies. European Journal of Neurology. 2016; 23: 1001–1019. https://doi.org/10.1111/ene.13002.
- [18] Huang Z, Jiang C, Li L, Xu Q, Ge J, Li M, et al. Correlations between dopaminergic dysfunction and abnormal metabolic network activity in REM sleep behavior disorder. Journal of Cerebral Blood Flow and Metabolism: Official Journal of the International Society of Cerebral Blood Flow and Metabolism. 2020; 40: 552–562. https://doi.org/10.1177/0271678X19828916.



- [19] Ma Y, Tang C, Spetsieris PG, Dhawan V, Eidelberg D. Abnormal metabolic network activity in Parkinson's disease: test-retest reproducibility. Journal of Cerebral Blood Flow and Metabolism: Official Journal of the International Society of Cerebral Blood Flow and Metabolism. 2007; 27: 597–605. https://doi.org/10.1038/sj.jcbfm.9600358.
- [20] Ma Y, Tang C, Chaly T, Greene P, Breeze R, Fahn S, et al. Dopamine cell implantation in Parkinson's disease: long-term clinical and (18)F-FDOPA PET outcomes. Journal of Nuclear Medicine: Official Publication, Society of Nuclear Medicine. 2010; 51: 7–15. https://doi.org/10.2967/jnumed.109.066811.
- [21] Jiang L, Wang X, Li P, Feng Z, Shi X, Shao H. Efficacy of 11C-2β-carbomethoxy-3β-(4-fluorophenyl) tropane positron emission tomography combined with 18F-fluorodeoxyglucose positron emission tomography in the diagnosis of early Parkinson disease: A protocol for systematic review and meta analysis. Medicine. 2020; 99: e23395. https://doi.org/10.1097/MD 00000000000023395.
- [22] Bloem BR, Okun MS, Klein C. Parkinson's disease. Lancet (London, England). 2021; 397: 2284–2303. https://doi.org/10. 1016/S0140-6736(21)00218-X.
- [23] Xu J, Xu Q, Liu S, Li L, Li L, Yen TC, et al. Computer-Aided Classification Framework of Parkinsonian Disorders Using ¹¹C-CFT PET Imaging. Frontiers in Aging Neuroscience. 2022; 13: 792951. https://doi.org/10.3389/fnagi.2021.792951.
- [24] Sun X, Liu F, Liu Q, Gai Y, Ruan W, Wimalarathne DN, *et al.* Quantitative Research of ¹¹C-CFT and ¹⁸F-FDG PET in Parkinson's Disease: A Pilot Study With NeuroQ Software. Frontiers in Neuroscience. 2019; 13: 299. https://doi.org/10.3389/fnins. 2019.00299.
- [25] Jackson H, Anzures-Cabrera J, Taylor KI, Pagano G, PASADENA Investigators, Prasinezumab Study Group. Hoehn and Yahr Stage and Striatal Dat-SPECT Uptake Are Predictors of Parkinson's Disease Motor Progression. Frontiers in Neuroscience. 2021; 15: 765765. https://doi.org/10.3389/fnins.2021.765765.
- [26] Lorio S, Sambataro F, Bertolino A, Draganski B, Dukart J. The Combination of DAT-SPECT, Structural and Diffusion MRI Predicts Clinical Progression in Parkinson's Disease. Frontiers in Aging Neuroscience. 2019; 11: 57. https://doi.org/10.3389/fnag i.2019.00057.
- [27] Rosano C, Metti AL, Rosso AL, Studenski S, Bohnen NI. Influence of Striatal Dopamine, Cerebral Small Vessel Disease, and Other Risk Factors on Age-Related Parkinsonian Motor Signs.

- The Journals of Gerontology. Series A, Biological Sciences and Medical Sciences. 2020; 75: 696–701. https://doi.org/10.1093/gerona/glz161.
- [28] Booij J, Tissingh G, Winogrodzka A, Boer GJ, Stoof JC, Wolters EC, et al. Practical benefit of [123I]FP-CIT SPET in the demonstration of the dopaminergic deficit in Parkinson's disease. European Journal of Nuclear Medicine. 1997; 24: 68–71. https://doi.org/10.1007/BF01728311.
- [29] Tissingh G, Booij J, Bergmans P, Winogrodzka A, Janssen AG, van Royen EA, et al. Iodine-123-N-omega-fluoropropyl-2beta-carbomethoxy-3beta-(4-iod ophenyl)tropane SPECT in healthy controls and early-stage, drug-naive Parkinson's disease. Journal of Nuclear Medicine: Official Publication, Society of Nuclear Medicine. 1998; 39: 1143–1148.
- [30] Benamer HT, Patterson J, Wyper DJ, Hadley DM, Macphee GJ, Grosset DG. Correlation of Parkinson's disease severity and duration with 123I-FP-CIT SPECT striatal uptake. Movement Disorders: Official Journal of the Movement Disorder Society. 2000; 15: 692–698. https://doi.org/10.1002/1531-8257(200007)15:4<692::aid-mds1014>3.0.co;2-v.
- [31] Wen W, Piao Y, Xu D, Li X. Prognostic Value of MTV and TLG of ¹⁸F-FDG PET in Patients with Stage I and II Non-Small-Cell Lung Cancer: a Meta-Analysis. Contrast Media & Molecular Imaging. 2021; 2021: 7528971. https://doi.org/10.1155/2021/7528971.
- [32] Kaymak ZA, Karahan N, Erdoğan M, Erdemoğlu E, Zihni İ, Şengül SS. Correlation of ¹⁸F-FDG/PET SUV_{max}, SUV_{mean}, MTV, and TLG with HIF-1α in Patients with Colorectal Cancer. Molecular Imaging and Radionuclide Therapy. 2021; 30: 93–100. https://doi.org/10.4274/mirt.galenos.2021.04934.
- [33] Troiano AR, Schulzer M, de la Fuente-Fernandez R, Mak E, McKenzie J, Sossi V, et al. Dopamine transporter PET in normal aging: dopamine transporter decline and its possible role in preservation of motor function. Synapse (New York, N.Y.). 2010; 64: 146–151. https://doi.org/10.1002/syn.20708.
- [34] Ishibashi K, Oda K, Ishiwata K, Ishii K. Comparison of dopamine transporter decline in a patient with Parkinson's disease and normal aging effect. Journal of the Neurological Sciences. 2014; 339: 207–209. https://doi.org/10.1016/j.jns.2014. 01.015.
- [35] Kangli F, Hongguang Z, Yinghua L, Xiaoxiao D, Yuyin D, Lulu G, et al. Characteristics and influencing factors of ¹¹C-CFT PET imaging in patients with early and late onset Parkinson's disease. Frontiers in Neurology. 2023; 14: 1195577. https://doi.org/10.3389/fneur.2023.1195577.

